

## Quantification of Nanoparticle Release from Polymer Nanocomposite Coatings due to Environmental Stressing

Yeon Seok Kim, Rick Davis, Nasir Uddin, Marc Nyden & Savelas A. Rabb

To cite this article: Yeon Seok Kim, Rick Davis, Nasir Uddin, Marc Nyden & Savelas A. Rabb (2015): Quantification of Nanoparticle Release from Polymer Nanocomposite Coatings due to Environmental Stressing, Journal of Occupational and Environmental Hygiene, DOI: 10.1080/15459624.2015.1116696

To link to this article: <http://dx.doi.org/10.1080/15459624.2015.1116696>

 View supplementary material 

 Accepted author version posted online: 08 Dec 2015.

 Submit your article to this journal 

 Article views: 29

 View related articles 

 View Crossmark data 

## **Quantification of Nanoparticle Release from Polymer Nanocomposite Coatings due to Environmental Stressing**

Yeon Seok Kim\*, Rick Davis, Nasir Uddin, Marc Nyden, and Savelas A. Rabb,

National Institute of Standards and Technology, 100 Bureau Drive MS-8665, Gaithersburg, MD  
20899-8665, USA

\*Person to whom correspondence should be addressed.

E-mail address: [yeonkim@nist.gov](mailto:yeonkim@nist.gov)

**Keywords:** Engineered Nanoparticle; UV-Vis; ICP-OES; Simulated Chewing; Simulated Wear and tear; Layer-by-Layer Assembly

**Exposition Word Count:** 4239

## ABSTRACT

Certain engineered nanoparticles (ENP) reduce the flammability of components used in soft furnishings (mattresses and upholstered furniture). However, because of the ENP's small size and ability to interact with biological molecules, these fire retardant ENPs may pose a health and environmental risks, if they are released sometime during the life cycle of the soft furnishing. Quantifying the released amount of these ENPs under normal end-use circumstances provides a basis for assessing their potential health and environmental impact. In this manuscript, we report on efforts to identify suitable methodologies for quantifying the release of carbon nanofibers, carbon nanotubes, and sodium montmorillonites from coatings applied to the surfaces of barrier fabric and polyurethane foam. The ENPs released in simulated chewing and mechanical stressing experiments were collected in aqueous solution and quantified using Ultraviolet-Visible and inductively coupled plasma–optical emission spectroscopy. The microstructures of the released ENPs were characterized using scanning electron microscopy. The reported methodology and results provide important milestones to estimate the impact and toxicity of the ENP release during the life cycle of the nanocomposites. To our knowledge, this is the first study of ENP release from the soft furnishing coating, can be important application area for fire safety.

## INTRODUCTION

Soft furnishings fires (mattresses and upholstered furniture) only account for 5 % of the 385,100 annual residential fires in the United States.<sup>(1)</sup> Soft furnishings fires, however, result in a disproportionately high fraction of fire losses (33 % of the civilian fatalities, 18 % of civilian injuries, and 11 % of the property losses).<sup>(1-3)</sup> Flame retardant (FR) chemicals, such as halogenated and phosphorous FRs, are used in a wide variety of products including soft furnishings to reduce the fire threat and comply with fire regulations. However, due to concerns about their effectiveness and potential negative environmental and health impact, manufactures are searching for alternative FR solutions.<sup>(4-7)</sup>

During the last two decades, engineered nanoparticles (ENPs) have been studied as a FR for polymers.<sup>(8-16)</sup> ENPs are typically incorporated directly in the polymer as an additive, forming a network structure within the polymer matrix. This network hinders the release of combustible gases by creating a physically blocking layer on the surface during the pyrolysis/combustion process.<sup>(16,17)</sup> There are, however, several drawbacks hindering ENPs as a replacement for existing FR chemicals such as high cost, the ENP handling, and complicate fabrication process. Another drawback is that these ENPs have a delayed effect (the time it takes to form a fire blocking layer on the surface), which may result in an initial rapid flame spread.<sup>(16,17)</sup>

More recently, ENPs have been applied on the surface of, rather than inside, polymeric substrates using Layer-by-Layer (LbL) assembly.<sup>(18-30)</sup> These thin multilayer

ENP filled coatings are constructed by alternative depositions of oppositely charged polyelectrolytes and/or ENP layers. Various ENPs including, carbon nanofiber (CNF),<sup>(18)</sup> multi-walled carbon nanotube (MWCNT),<sup>(31)</sup> polyhedral oligomeric silsesquioxanes,<sup>(32)</sup> silica,<sup>(22)</sup>  $\alpha$ -zirconium phosphate,<sup>(21)</sup> and sodium montmorillonite (MMT),<sup>(23-25)</sup> were deposited on various substrates such as textiles,<sup>(26,32)</sup> plastic films,<sup>(27-29)</sup> and flexible polyurethane foams (PUF).<sup>(18,23,30)</sup> These coatings show excellent fire resistance; e.g., up to 70% reduction in PUF flammability and self-extinguishment on cotton fabric. Presumably, this is because all the ENPs are concentrated at the surface, which enables rapid formation of a blocking layer.

ENPs FR may pose health and environmental risks if released during routine end-use stresses (e.g., cleaning, chewing, and normal wear-and-tear). Because of its small size, released ENPs can be introduced into the human body by inhalation, ingestion, and skin penetration.<sup>(33-37)</sup> ENP-filled LbL coatings may have a greater chance of releasing the ENPs, since all the ENPs are located on the surface rather than bound within the substrate. The health risk of ENPs is estimated by the ENP toxicity and exposure level. Most studies have focused on the toxicity of ENPs based on the assumption of a high ENP exposure level.<sup>(34,38)</sup> To more accurately estimate the risk and effects of ENPs on human health and the environment, it is necessary to develop a methodology to simulate and measure the release of ENPs during the normal use life cycle.

In this manuscript, we report on efforts to identify suitable methodologies for quantifying the release of MMT, MWCNT, and CNF. These ENPs were contained in thin FR coatings on flexible polyurethane foam (PUF) and barrier fabrics (BF). The ENPs

were released as a result of simulated chewing (e.g., by a toddler) and wear-and-tear mechanical stressing performed with a head-over-heels (HOH) extractor and mechanical pounding (MP).<sup>(39)</sup> This is the first, of what is expected to be a series of studies focusing on the development of test methods for assessing the risk of exposure to ENPs incurred during routine use of products containing ENP FRs.

## MATERIALS AND METHODS<sup>†, ††</sup>

### Materials

All materials were used as-received from the supplier unless otherwise indicated. Branched polyethylenimine (PEI, branched, Mw = 25,000 g/mol), poly (acrylic acid) (PAA, Mw= 100,000 g/mol) and sodium dodecyl sulfate (SDS) were obtained from Sigma-Aldrich (Milwaukee, WI). Baytubes C150HP multi-walled carbon nanotube (MWCNT, average diameter = 14 nm, length = 1  $\mu$ m to 10  $\mu$ m) were obtained from Bayer MaterialScience AG (Pittsburgh, Pennsylvania). PR-24-XT-PS carbon nanofibers (CNF, average diameter = 100 nm, length = 30  $\mu$ m to 100  $\mu$ m) were obtained from Pyrograf Products Inc. (Cedarville, OH). These CNF were pretreated by manufacturer to improve the dispersion in aqueous solution. Sodium montmorillonite (MMT, trade name is Cloisite Na+) was obtained from Southern Clay Products Inc. (Gonzales, TX). The flexible polyurethane (PUF) obtained from Future Foam Inc. (Fullerton, CA) and was

stored as-received. The barrier fabric (BF) was a poly(melamine-co-formaldehyde) based nonwoven (density of 222 g/m<sup>2</sup>) from Basofil Fibers LLC. (Greensboro, NC).

### Preparation of Coating Solutions

The polyelectrolyte solutions ( $0.10 \pm 0.03$  mass %) were prepared with deionized water (DI) and either PAA or PEI, then tumbled for 12 h at room temperature using a compact roller system manufactured by Wheaton (Millville, NJ). Three different ENP suspensions were used for deposition. Different ENP concentrations were selected to match the final coating mass and the ENP concentration in the coating. The CNF suspensions were prepared by adding  $0.05 \pm 0.01$  mass % of CNF into  $0.10 \pm 0.01$  mass % PEI solution then sonicated at 40 W for 1 hr. MWCNTs were first functionalized via a direct amination method in order to improve the stability in water.<sup>(31)</sup> After the surface functionalization, MWCNTs were able to disperse in water without any dispersion agent. Functionalized MWCNTs solution ( $0.10 \pm 0.01$  mass %) was added to Deionized (DI) water then sonicated at 40 W for 1 hr. The CNF and MWCNT suspensions were used immediately after preparation. The MMT suspension was prepared by adding  $0.20 \pm 0.01$  mass % of MMT to DI water then rolling overnight to disperse the MMT.

### LbL Assembly Coating Fabrication

Prior to coating, the substrate (PUF and BF) was stored in a desiccator for two days to remove moisture (necessary for calculating the coating mass). The mass of each substrate

was measured immediately before the deposition process. All the ENP coatings were fabricated by alternate absorption of polyelectrolyte and ENP monolayers. Three different coatings were applied, 4 bi-layer (BL) of CNF, 4 tri-layer (TL) of MWCNT, and 8 TL of MMT (Scheme 1). Each monolayer was deposited by soaking the substrate in the deposition solution for a specific time (5 min for each monolayer in the first BL or TL, and 1 min for each subsequent monolayer) until the desired number of layers were deposited. After coating, the substrates were placed in a  $70 \pm 1$  °C convection oven overnight, then stored in a desiccator for two days to remove any remaining water. The coating mass is the difference between the mass of the substrate prior to coating and the mass of the coated substrate. Both mass measurements were made after the substrate was stored in a desiccator. More details of the fabrication are found elsewhere.<sup>(18,19,23)</sup>

### Specimen Stressing

A custom built Tissue Culture Rotator (Head-over-Heels shaker, HOH) was used to simulate the type of stresses expected from a toddler “chewing” on a soft furnishing.<sup>(39)</sup> Each coated specimen was cut into 16 small pieces ( $1.0 \pm 0.2$  g for PUF,  $0.25 \pm 0.05$  g for BF). Four specimen pieces were placed in each of the four polymer coated glass bottles. These glass bottles contained 100 mL simulated saliva ( $0.90 \pm 0.05$  mass % NaCl in deionized water). The bottles were positioned  $8.0 \text{ cm} \pm 0.1 \text{ cm}$  from the horizontal turning shaft of the HOH. The bottles spun at a rate of 1 rev/sec for 30 min. The samples were removed after squeezing the liquid back into the bottle. This process was repeated a total of 10 times using the same extraction solvent, so the resulting extractions were from the

accumulation of 10 coated PUF or BF samples. This approach, using the same extraction solution for 10 samples, was necessary to ensure that the ENP concentration was above the detection limit in the UV-Vis.

An in-house pneumatic mechanical pounder (MP) was used to simulate the “wear and tear” expected from routine use of soft furnishings for five years.<sup>(39)</sup> The pounding element is a convex shaped head made from hard plastic (diameter of  $8.9 \text{ cm} \pm 0.1 \text{ cm}$ ) that was driven by a pneumatic (vertical) piston. A test specimen was placed in a polyolefin bag, then secured under the pounder by set screws positioned around the edge of the substrate. The BF specimen was placed on top of untreated PUF to reflect the component layering observed in commercial soft furnishings. The specimen was subjected to 100,000 pounding cycles (approximately 28 h) at a frequency of 1 cycle/s exerting a force (pressure) of  $20,682 \pm 69 \text{ Pa}$ . After the pounding was complete, the specimen was removed from the bag. The bag was then washed with deionized water (100 mL) that contained  $0.23 \pm 0.02 \text{ mass \% SDS}$ . This process was repeated 10 times, using the same wash suspension for each specimen type, so that the wear and tear washing used in quantifying the release was from 10 coated PUF or BF specimens. Similar to the simulated chewing test, using the same extraction solution for the 10 samples was necessary to ensure that the ENP concentration was above the detection limit of the UV-Vis.

### Measurements Methodology

The amount of released CNFs and MWCNTs was quantified by absorption spectroscopy in the ultraviolet-visible (UV-Vis) region. Prior to the measurement, NaCl in the extracted solutions was removed by dialysis because NaCl was causing ENP agglomeration. A 50 ml aliquot of each suspension was transferred to a Pierce Snakeskin pleated dialysis tube (10,000 g/mol molecular weight cut-off). The tube was suspended in a beaker containing approximately 2 L of DI water. The conductivity of the water in the beaker was monitored and frequently replaced with fresh DI water. The dialysis continued until the conductivity of the beaker water reached to that of pure DI water ( $< 0.5 \mu\text{S}$ ) over a 2 hr period. Dialysis process generally took 24 hr. A small amount of the extraction solution was lost during dialysis. This was corrected by calculating the ENP concentration by scaling the ratios of the initial mass of extraction solution (typically, about 50 g) to the post dialysis mass (typically, between 45 g and 49 g). After dialysis, the solutions were sonicated at 50 W for 1 h prior to the measurement to help create a well-dispersed and stable ENP suspension.

The amount of released MMTs was measured using inductively coupled plasma–optical emission spectroscopy (ICP-OES). The measurements were made using a Perkin Elmer Optima 5300 DV ICP-OES (Shelton, CT). Magnesium (Mg) was selected to quantify the amount of released MMT. Two external calibrations were generated using the MMT starting material. NaCl (0.2 mass %) was added to one set of standards to match the sample matrix of the HOH extractions. Mg was measured at the excitation wavelength of 279.5 nm. ENP coatings and released ENPs in the extracted solution were also characterized by a Zeiss Ultra 60 Field Emission-Scanning Electron Microscope (FE-

SEM, Carl Zeiss Inc., Thornwood, NY) under 5 kV accelerating voltage. All SEM samples were sputter coated with 5 nm of Au/Pd (60 %/40 % by mass) prior to SEM imaging.

## RESULTS AND DISCUSSION

Each ENP used in this study has distinct characteristics in size and configuration so it was necessary to develop separate methodology to measure each ENP release. Fortunately, CNF and MWCNT can be measured with identical methodology despite the size difference of them. All ENP releases from 12 different situations were measured using two different methodologies: one for CNF and MWCNT and one for MMT. Following sections will discuss each methodology and characterization results.

### Quantifying CNF and MWCNT Release

The release of CNFs and MWCNTs were measured using UV-Vis spectroscopy. This technique is commonly used to estimate carbon nanotube dispersion<sup>(40,41)</sup> and concentration<sup>(42-45)</sup> in a suspension. A representative UV-Vis spectrum of a MWCNT suspension (after subtracting the background spectrum of the SDS solution) is provided in supporting information. The nanoparticle concentration is based on the absorbance intensity at the wavelength of 267 nm for the maximum CNF and MWCNT absorbance value.

Nanoparticle dispersion and stabilization is critical to the UV-Vis measurement. The UV-Vis absorbance intensity is related to the nanoparticle surface area that is strongly affected by the nanoparticle dispersion. Therefore poor ENP dispersion lowers the absorbance intensity even with same ENP concentration. Poor ENP dispersion also impacts the ENP stability, which also influence the UV-Vis absorbance. Unstable nanoparticles will aggregate and precipitate out of solution eventually. The result is the UV-Vis absorbance intensity value will decrease over time, which can happen in a short time depending on the stability level. The result is an unreliable absorbance value (nanoparticle concentration) that is dependent of time between sample preparation and analysis.

A dispersion and stability problem was encountered in the CNF and MWCNT analysis even though both of them are pretreated to improve a dispersion and stability. Initially, the CNF and MWCNT concentration was measured directly from the simulated saliva solution. Even after adding a stabilizing surfactant (0.23 mass % SDS in DI water),<sup>(46)</sup> the CNF and MWCNT suspensions were visually unstable and resulted in absorbance values that changed significantly over time. The  $0.9 \pm 0.05$  mass % NaCl in the simulated saliva solution caused the MWCNTs and CNFs to aggregate, which led to the observed instability.

NaCl was completely removed by dialysis to improve the stability of the suspensions. Figure 1 shows the impact of NaCl and removing NaCl on the UV-Vis absorbance intensity value. The UV-Vis spectrum for a  $0.005 \pm 0.0003$  mass % CNF suspension without NaCl has an absorbance value of 2.18 at 267 nm. When NaCl was added, the

absorbance value decreased to 1.66 due to CNF aggregation. The NaCl was then removed by dialysis, and the absorbance value became similar ( $2.16 \pm 0.10$ , after dialysis spectrum) to the solution prepared without any NaCl. Our conclusion is that NaCl caused CNF aggregation, but with the combination of dialysis and SDS, the UV-Vis absorbance values were an accurate and repeatable measure of the CNF concentration. The same behavior and mitigation strategy was used for the MWCNT solution.

Based on these findings, all of the simulated chewing extractions containing MWCNTs or CNFs were prepared for UV-Vis analysis using the following steps: 1) dialysis until a conductivity become less than  $0.5 \mu\text{S}$  (~24 hr), 2) add 0.23 mass % SDS to stabilize the nanoparticles, and 3) sonicate for 1 h at 40 W to create a well-dispersed and distributed nanoparticle suspension. The wear-and-tear washings were prepared using this same procedure except no dialysis was required since NaCl was not present.

The CNF and MWCNT concentrations in all of the simulated chewing extractions and wear and tear washings were determined from Beer's Law calibration curves. The absorbance values at the maximum of the absorbance band (267 nm) from five calibration suspensions were fit to a straight line. The calibration suspensions were prepared by diluting aliquots taken from a master suspension. Figures 2 and 3 are the Beer's Law curves for CNFs and MWCNTs calibration suspensions, respectively. The calibration curve of CNF suspensions after dialysis is nearly identical to the curve of the sodium chloride free suspensions. Although the dialysis appears to be less effective for MWCNT (figure 3), the difference in the calibration curves is small at the lower concentration region, which is the concentration range for the extractions and washings. The  $2\sigma$

standard uncertainty of the concentrations obtained from these calibration curves was  $\pm 5\%$  of the CNF or MWCNT mass % value. The lower limit of detection was  $0.00010 \pm 0.00005$  mass %.

### Quantifying MMT Release

The release of MMT was measured by elemental analysis using ICP-OES. MMT contains metals such as Al, Fe, Mg, and Na. The amount of each of these metals present in the MMT was determined by adding known amounts of these metals to a dilute  $\text{HNO}_3$  solution containing  $0.002 \pm 0.0001$  mass % MMT. The measured ICP-OES intensities at the wavelengths of 394 nm (Al), 234 nm (Fe), 285 nm (Mg), and 589 nm (Na) for solutions containing 5 concentrations of each element are shown in Figure 4. The concentration of each metal in MMT was obtained by dividing the measured intensity at zero added metal (y-intercept) by the slope of the corresponding line (provided in supporting information).

Mg was selected to quantify MMT since it had better sensitivity and precision than the other elements. During the analyses, the ICP-OES signals were observed to be significantly enhanced in the presence of NaCl. Thus different calibration curves were needed for the quantitative analysis of the simulated chewing extractions that contained NaCl. These calibration curves for Mg are shown in Figure 5. A series of 3 standards were prepared by diluting aliquots of known volume from a master suspension containing  $0.002 \pm 0.0001$  mass % MMT (in dilute  $\text{HNO}_3$ ) and adding  $0.2 \pm 0.01$  mass % NaCl to the standards used in quantifying the MMT in the extractions. The samples obtained from the extractions were then diluted prior to the analyses (from 0.9 mass % to 0.2 mass % NaCl) to ensure that the concentration of NaCl was the same as the calibration standards.

### **ENP Release Comparison**

The amounts of ENPs released are reported in Table I for the simulated wear and tear stressing and Table II for the simulated chewing stress. The quantities of ENP are expressed as a percentage of the total ENP content as well as the total mass of ENP collected. The quantity as a percentage of the total ENP content reflects the durability of the ENP coating; a higher percentage means the ENP was more easily released. The total mass of the collected ENP depends on the mass of the coating as well as coating durability. High ENP quantities can result from a lot of ENPs released from a thin, low durability coating or a few of ENPs released from a thick, high durability coating.

The quantity as a percentage of the total ENP helps to understand the release scenario, and the total mass of collected ENPs is important to estimate the exposure risk of these ENP coatings. The exposure risk mainly depends on the amount collected, not the release scenario.

Regardless of the ENP type, the amount of ENPs released from wear-and-tear stressing was higher from the BF than the PUF. During wear-and-tear, the BF tended to fragment into smaller pieces. These pieces were suspended in the wear-and-tear washing solution along with imbedded ENPs. Therefore, the higher release values may be a consequence of the BF being more susceptible to mechanical stresses than the PUF.

Regardless of the substrate type, the amount of ENPs released from wear-and-tear stressing was dependent on the type of ENP. The amount of ENPs released was as follows: CNF > MWCNT >> MMT. This ordering reflects the relative durability of ENP in the coatings. Since the coatings are constructed of the same polymeric materials (PEI and PAA), the durability is related to the ability of the ENPs to interact with the polymeric layers in the coating. The data suggests MMT likely adheres better to the polymeric layers, which results in more durable coating than other ENPs coatings. This behavior can be explained by the different construction mechanism between MMT and MWCNT/CNF coatings. During the deposition process, MMT platelets are stacked on top of each other like a brick wall. This creates a more ordered structure that is durable under one directional mechanical stressing. On the other hand, CNFs and MWCNTs form a 3-dimensional network structure within the coating that is less durable under one directional

stressing. The difference between CNF and MWCNT coatings may result from the size differences and surface treatment of CNFs and MWCNTs.

The ENP coatings are much less durable in the simulated chewing stressing. The amount of ENPs released from the simulated chewing is approximately an order of magnitude higher than measured from the simulated wear-and-tear stressing. However, there were similar trends, such as the ENPs released from the BFs were higher than from the PUFs. The one exception is that the MWCNTs released from the chewing stressing were statistically the same for the BF and PUF. Similar to the wear-and-tear stressing, the amount of ENPs released from the simulated chewing was also dependent on the type of ENP. Regardless of the substrate type, the amount of ENPs released was as follows: MWCNT >> CNF ~ MMT. These results suggest that the ENP coatings are more susceptible to ionic solution, such as the simulated saliva, than mechanical stressing. The salt water likely caused the coating to swell and separate from the substrate. The hierarchy of ENP released is then based on the affinity of the ENP to the coating and the polymer. Apparently, MWCNT has the highest affinity due to the surface functionalization resulting in higher release rate for simulated chewing.

The ENP release behavior is strongly influenced by the coating microstructure (Figure 6). There are a lot of CNFs that are loosely bound to the polymeric matrix and not embedded in the coating as shown in Figure 6 (a) and (b). The size of these exposed CNFs can be up to 50  $\mu\text{m}$ . These attributes make the coating more susceptible to mechanical stress release of the ENP. However, these attributes may have little impact on

release in the simulated saliva because the CNFs don't have a strong affinity for the salt solution resulting in lower release rate for simulated chewing.

The MWCNTs and MMTs produce more cohesive coatings (Figure 6 (c) – 6 (f)). Both MWCNTs and MMTs have large surface area and strong attraction to polymer resulting in a smooth coating, smaller aggregates, and all the ENPs being completely embedded in the polymeric layers. These attributes make these coating more durable (than CNF) to mechanical stressing. The MMT smaller aggregate size and 2-dimensional geometry explains why the MMT coating has the lowest release rate among the three ENP coatings.

### **Released ENP Microstructure**

The amount and the form of the released ENPs into the environment are key factors in determining health risk. Free ENPs may be more easily absorbed into the human body because they are truly in nanoscale and tend to have high reactivity. ENPs bound to the polymeric matrix or substrate has, however, less toxicity due to their larger size and lower reactivity.

In order to understand the released ENP configuration, airborne released particles were captured and characterized using SEM. All airborne particles were captured by placing a polycarbonate filter paper connected to a pump near the pounding station located in an enclosed case. Only wear-and-tear released particles were collected and characterized. Simulated chewing released particles were not characterized by SEM, because the released particles crystalized and aggregated due to the presence of NaCl in saline solution (supporting information). These microstructure images confirm that it is

necessary to pretreat the extracted solution as described in previous section to ensure the accurate measurement. Without dialysis the released ENPs are crystalized due to NaCl, and without strong sonication ENPs are highly aggregated as shown in SEM images.

Due to the mechanical stress, a portion of the coating was delaminated from the substrate and became airborne particles. The released particle size from the MWCNT and MMT coatings varied from less than one micron to tens of microns (Figure 7(a) and (b)). These particles are substantially larger than these ENPs, which are less than 150 nm. This suggests that the released MWCNTs and MMTs were embedded in the polymer matrix when released. No free MWCNTs and MMTs were observed. However, out of five tests we observed two free CNFs (Figure 7 (c) and (d)).

These results are well aligned with characterization of the coating microstructure. MWCNTs and MMTs exhibit good adhesion with the polymeric layers and all MWCNTs and MMTs are completely embedded into the polymer matrix. In contrast, CNFs have relatively weak adhesion with polymeric layers due to its larger size and less surface area, and some of the CNFs were not even embedded in the coating.<sup>(18)</sup> This creates a higher probability for the CNFs to be released from the coating.

Obviously strong bonding between ENP and the matrix is important to retain ENPs within the polymer matrix, even after they are released into the environment. It is worth noting that the size of CNFs is still comparable to the released particles from other coatings. Without further study of the toxicity of these particles, it is premature to conclude that CNFs are more of a health risk than other ENPs in this study.

## CONCLUSIONS

In this manuscript we described and used methodologies for releasing, measuring, and characterizing MMTs, MWCNTs, and CNFs released from coatings on BF and PUF. Three ENPs were successfully deposited on two different substrates. The coated substrates were stressed to simulate normal wear-and-tear and chewing by a toddler. The released ENPs were collected in aqueous suspensions and quantified using UV-Vis and ICP-OES. The UV-Vis analyses provided reliable and accurate estimates of the CNFs and MWCNTs. ICP-OES analyses was more suitable to quantify the amount of released MMTs. Critical to the accuracy and repeatability of these measurements was removing NaCl by dialysis, which caused ENP aggregation.

For the normal wear-and-tear stressing, MMTs released was the lowest and CNFs released was the highest. For the simulated chewing stressing, MWCNTs released was significantly higher because of its greater compatibility with the simulated saliva. SEM images show that most of the ENPs still remain in the polymer matrix, except a couple of CNFs were observed from the wear-and-tear stressing. Future studies will be performed to estimate the toxicity of the released ENPs. The ENPs release under the different types of stressing including UV aging, laundry, and elevated temperature will be evaluated also.

## ACKNOWLEDGMENT

The authors thank Dr. Jeffrey Fagan for consulting and helping UV-Vis measurement. This work was partially supported by Consumer Product Safety Commission. Dr. Uddin personally thanks for National Research Council Research Associateship Program.

## Notes

† NIST, Certain commercial equipment, instruments or materials are identified in this paper in order to specify the experimental procedure adequately. Such identification is not intended to imply recommendation or endorsement by the National Institute of Standards and Technology, nor is it intended to imply that the materials or equipment identified are necessarily the best available for this purpose.

†† NIST, The policy of NIST is to use metric units of measurement in all its publications, and to provide statements of uncertainty for all original measurements. In this document, however, data from organizations outside NIST are shown, which may include measurements in non-metric units or measurements without uncertainty statements.

## REFERENCE

- 1 **Miller, D., R. Chowdhury, and M. Greene:** "2005-2007 Residential Fire Loss Estimates." [Online] Available at <http://www.cpsc.gov/library/fire07.pdf>, 2010).
- 2 **Ahrens, M.:** "Home Fires That Began With Upholstered Furniture". Quincy, MA: National Fire Protection Association, 2011.

- 3 **Evarts, B.:** *Home Fires That Began With Mattresses and Bedding*. Quincy, MA: National Fire Protection Association, 2011.
- 4 **Blum, A., and B. Ames:** Flame-retardant additives as possible cancer hazards. *Science* 195(4273): 17-23 (1977).
- 5 **Birnbaum, L.S., and D.F. Staskal:** Brominated flame retardants: Cause for concern? *Environmental Health Perspectives* 112(1): 9-17 (2004).
- 6 **Cordner, A., M. Mulcahy, and P. Brown:** Chemical Regulation on Fire: Rapid Policy Advances on Flame Retardants. *Environmental Science & Technology* (2013).
- 7 **Stapleton, H.M., S. Klosterhaus, S. Eagle, J. Fuh, J.D. Meeker, A. Blum et al.:** Detection of Organophosphate Flame Retardants in Furniture Foam and U.S. House Dust. *Environmental Science & Technology* 43(19): 7490-7495 (2009).
- 8 **Gilman, J.W., T. Kashiwagi, and J.D. Lichtenhan:** Nanocomposites: A revolutionary new flame retardant approach. *Sampe Journal* 33(4): 40-46 (1997).
- 9 **Zammarano, M., R.H. Kramer, R. Harris, T.J. Ohlemiller, J.R. Shields, S.S. Rahatekar et al.:** Flammability reduction of flexible polyurethane foams via carbon nanofiber network formation. *Polymers for Advanced Technologies* 19(6): 588-595 (2008).
- 10 **Alexandre, M., and P. Dubois:** Polymer-layered silicate nanocomposites: preparation, properties and uses of a new class of materials. *Materials Science & Engineering R-Reports* 28(1-2): 1-63 (2000).
- 11 **Kashiwagi, T., E. Grulke, J. Hilding, R. Harris, W. Awad, and J. Douglas:** Thermal degradation and flammability properties of poly(propylene)/carbon nanotube composites. *Macromolecular Rapid Communications* 23(13): 761-765 (2002).

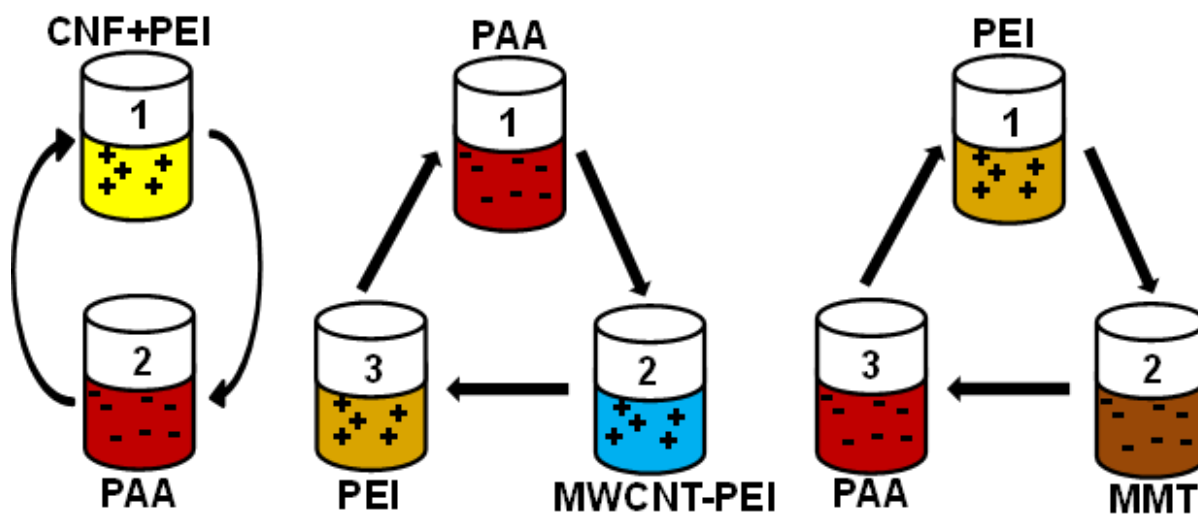
- 12 **Liu, Y.-L., C.-Y. Hsu, W.-L. Wei, and R.-J. Jeng:** Preparation and thermal properties of epoxy-silica nanocomposites from nanoscale colloidal silica. *Polymer* 44(18): 5159-5167 (2003).
- 13 **Kashiwagi, T., A.B. Morgan, J.M. Antonucci, M.R. VanLandingham, R.H. Harris, W.H. Awad et al.:** Thermal and flammability properties of a silica-poly(methylmethacrylate) nanocomposite. *Journal of Applied Polymer Science* 89(8): 2072-2078 (2003).
- 14 **Zhu, H.F., Q.L. Zhu, J.A. Li, K. Tao, L.X. Xue, and Q. Yan:** Synergistic effect between expandable graphite and ammonium polyphosphate on flame retarded polylactide. *Polymer Degradation and Stability* 96(2): 183-189 (2011).
- 15 **Becker, C.M., A.D. Gabbardo, F. Wypych, and S.C. Amico:** Mechanical and flame-retardant properties of epoxy/Mg-Al LDH composites. *Composites Part a-Applied Science and Manufacturing* 42(2): 196-202 (2011).
- 16 **Kashiwagi, T., F.M. Du, J.F. Douglas, K.I. Winey, R.H. Harris, and J.R. Shields:** Nanoparticle networks reduce the flammability of polymer nanocomposites. *Nature Materials* 4(12): 928-933 (2005).
- 17 **Zammarano, M., R.H. Krämer, R. Harris, T.J. Ohlemiller, J.R. Shields, S.S. Rahatekar et al.:** Flammability reduction of flexible polyurethane foams via carbon nanofiber network formation. *Polymers for Advanced Technologies* 19(6): 588-595 (2008).
- 18 **Kim, Y.S., R. Davis, A.A. Cain, and J.C. Grunlan:** Development of layer-by-layer assembled carbon nanofiber-filled coatings to reduce polyurethane foam flammability. *Polymer* 52(13): 2847-2855 (2011).

- 19 **Kim, Y.S., Y.-C. Li, W.M. Pitts, M. Werrel, and R.D. Davis:** Rapid Growing Clay Coatings to Reduce the Fire Threat of Furniture. *ACS Applied Materials & Interfaces* 6(3): 2146-2152 (2014).
- 20 **Li, Y.C., S. Mannen, J. Schulz, and J.C. Grunlan:** Growth and fire protection behavior of POSS-based multilayer thin films. *Journal of Materials Chemistry* 21(9): 3060-3069 (2011).
- 21 **Carosio, F., J. Alongi, and G. Malucelli:** alpha-Zirconium phosphate-based nanoarchitectures on polyester fabrics through layer-by-layer assembly. *Journal of Materials Chemistry* 21(28): 10370-10376 (2011).
- 22 **Laufer, G., F. Carosio, R. Martinez, G. Camino, and J.C. Grunlan:** Growth and fire resistance of colloidal silica-polyelectrolyte thin film assemblies. *Journal of Colloid and Interface Science* 356(1): 69-77 (2011).
- 23 **Kim, Y.S., R. Harris, and R. Davis:** Innovative Approach to Rapid Growth of Highly Clay-Filled Coatings on Porous Polyurethane Foam. *ACS Macro Letters* 1(7): 820-824 (2012).
- 24 **Li, Y.C., J. Schulz, S. Mannen, C. Delhom, B. Condon, S. Chang et al.:** Flame Retardant Behavior of Polyelectrolyte-Clay Thin Film Assemblies on Cotton Fabric. *ACS Nano* 4(6): 3325-3337 (2010).
- 25 **Li, Y.-C., Y.S. Kim, J. Shields, and R. Davis:** Controlling polyurethane foam flammability and mechanical behaviour by tailoring the composition of clay-based multilayer nanocoatings. *Journal of Materials Chemistry A* 1(41): 12987-12997 (2013).
- 26 **Alongi, J., F. Carosio, and G. Malucelli:** Influence of ammonium polyphosphate-/poly(acrylic acid)-based layer by layer architectures on the char formation in cotton, polyester and their blends. *Polymer Degradation and Stability* 97(9): 1644-1653 (2012).

- 27 **Laachachi, A., V. Ball, K. Apaydin, V. Toniazzo, and D. Ruch:** Diffusion of Polyphosphates into (Poly(allylamine)-montmorillonite) Multilayer Films: Flame Retardant-Intumescent Films with Improved Oxygen Barrier. *Langmuir* 27(22): 13879-13887 (2011).
- 28 **Apaydin, K., A. Laachachi, V. Ball, M. Jimenez, S. Bourbigot, V. Toniazzo et al.:** Polyallylamine–montmorillonite as super flame retardant coating assemblies by layer-by-layer deposition on polyamide. *Polymer Degradation and Stability* 98(2): 627-634 (2013).
- 29 **Carosio, F., A. Di Blasio, J. Alongi, and G. Malucelli:** Layer by layer nanoarchitectures for the surface protection of polycarbonate. *European Polymer Journal* 49(2): 397-404 (2013).
- 30 **Laufer, G., C. Kirkland, A.A. Cain, and J.C. Grunlan:** Clay–Chitosan Nanobrick Walls: Completely Renewable Gas Barrier and Flame-Retardant Nanocoatings. *ACS Applied Materials & Interfaces* 4(3): 1643-1649 (2012).
- 31 **Kim, Y.S., and R. Davis:** Multi-walled carbon nanotube layer-by-layer coatings with a trilayer structure to reduce foam flammability. *Thin Solid Films* 550(0): 184-189 (2014).
- 32 **Li, Y.-C., S. Mannen, J. Schulz, and J.C. Grunlan:** Growth and fire protection behavior of POSS-based multilayer thin films. *Journal of Materials Chemistry* 21(9): 3060-3069 (2011).
- 33 **Alvarez, P.J.J., V. Colvin, J. Lead, and V. Stone:** Research Priorities to Advance Eco-Responsible Nanotechnology. *ACS Nano* 3(7): 1616-1619 (2009).
- 34 **Sharifi, S., S. Behzadi, S. Laurent, M.L. Forrest, P. Stroeve, and M. Mahmoudi:** Toxicity of nanomaterials. *Chemical Society Reviews* 41(6): 2323-2343 (2012).
- 35 **Som, C., M. Berges, Q. Chaudhry, M. Dusinska, T.F. Fernandes, S.I. Olsen et al.:** The importance of life cycle concepts for the development of safe nanoproducts. *Toxicology* 269(2–3): 160-169 (2010).

- 36 **Benn, T.M., and P. Westerhoff:** Nanoparticle Silver Released into Water from Commercially Available Sock Fabrics. *Environmental Science & Technology* 42(11): 4133-4139 (2008).
- 37 **Nowack, B., J.F. Ranville, S. Diamond, J.A. Gallego-Urrea, C. Metcalfe, J. Rose et al.:** Potential scenarios for nanomaterial release and subsequent alteration in the environment. *Environmental Toxicology and Chemistry* 31(1): 50-59 (2012).
- 38 **Gottschalk, F., and B. Nowack:** The release of engineered nanomaterials to the environment. *Journal of Environmental Monitoring* 13(5): 1145-1155 (2011).
- 39 **Thomas, T.A., and P.M. Brundage:** "Quantitative Assessment of Potential Health Effects From the Use of Fire Retardant (FR) Chemicals in Mattresses". Bethesda, MD: U.S. Consumer Product Safety Commission, 2006.
- 40 **Chiang, I.W., B.E. Brinson, A.Y. Huang, P.A. Willis, M.J. Bronikowski, J.L. Margrave et al.:** Purification and characterization of single-wall carbon nanotubes (SWNTs) obtained from the gas-phase decomposition of CO (HiPco process). *Journal of Physical Chemistry B* 105(35): 8297-8301 (2001).
- 41 **Yu, J.R., N. Grossiord, C.E. Koning, and J. Loos:** Controlling the dispersion of multi-wall carbon nanotubes in aqueous surfactant solution. *Carbon* 45(3): 618-623 (2007).
- 42 **Huang, X.Y., R.S. McLean, and M. Zheng:** High-resolution length sorting and purification of DNA-wrapped carbon nanotubes by size-exclusion chromatography. *Analytical Chemistry* 77(19): 6225-6228 (2005).

- 43 **Sun, X., S. Zaric, D. Daranciang, K. Welsher, Y. Lu, X. Li et al.:** Optical properties of ultrashort semiconducting single-walled carbon nanotube capsules down to sub-10 nm. *Journal of the American Chemical Society* 130(20): 6551-6555 (2008).
- 44 **Khripin, C.Y., X.M. Tu, J. Howarter, J. Fagan, and M. Zheng:** Concentration Measurement of Length-Fractionated Colloidal Single-Wall Carbon Nanotubes. *Analytical Chemistry* 84(20): 8733-8739 (2012).
- 45 **Jiang, L.Q., L. Gao, and J. Sun:** Production of aqueous colloidal dispersions of carbon nanotubes. *Journal of Colloid and Interface Science* 260(1): 89-94 (2003).
- 46 **Haggenmueller, R., S.S. Rahatekar, J.A. Fagan, J.H. Chun, M.L. Becker, R.R. Naik et al.:** Comparison of the quality of aqueous dispersions of single wall carbon nanotubes using surfactants and biomolecules. *Langmuir* 24(9): 5070-5078 (2008).



**SCHEME 1.** Schematics of Layer-by-Layer deposition process of CNFs, MWCNTs, and MMTs on polyurethane foam and barrier fabric

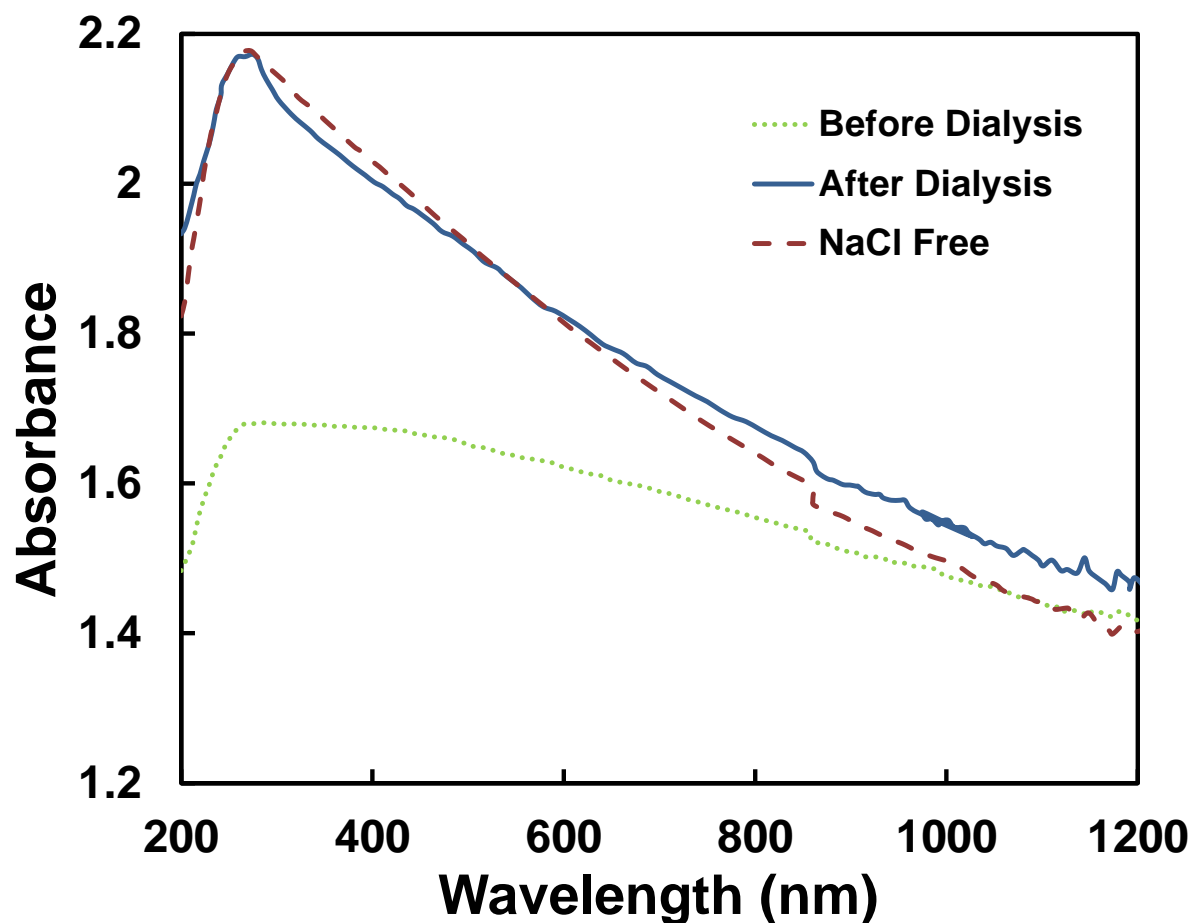


**FIGURE 1.** UV-Vis absorbance plot of a CNFs suspension prepared without sodium chloride, with sodium chloride, and the sodium chloride removed by dialysis. Dialysis was critical to obtaining accurate and repeatable absorbance values at the MWCNT and CNF peak maximum (267 nm) for the simulated chewing suspensions.

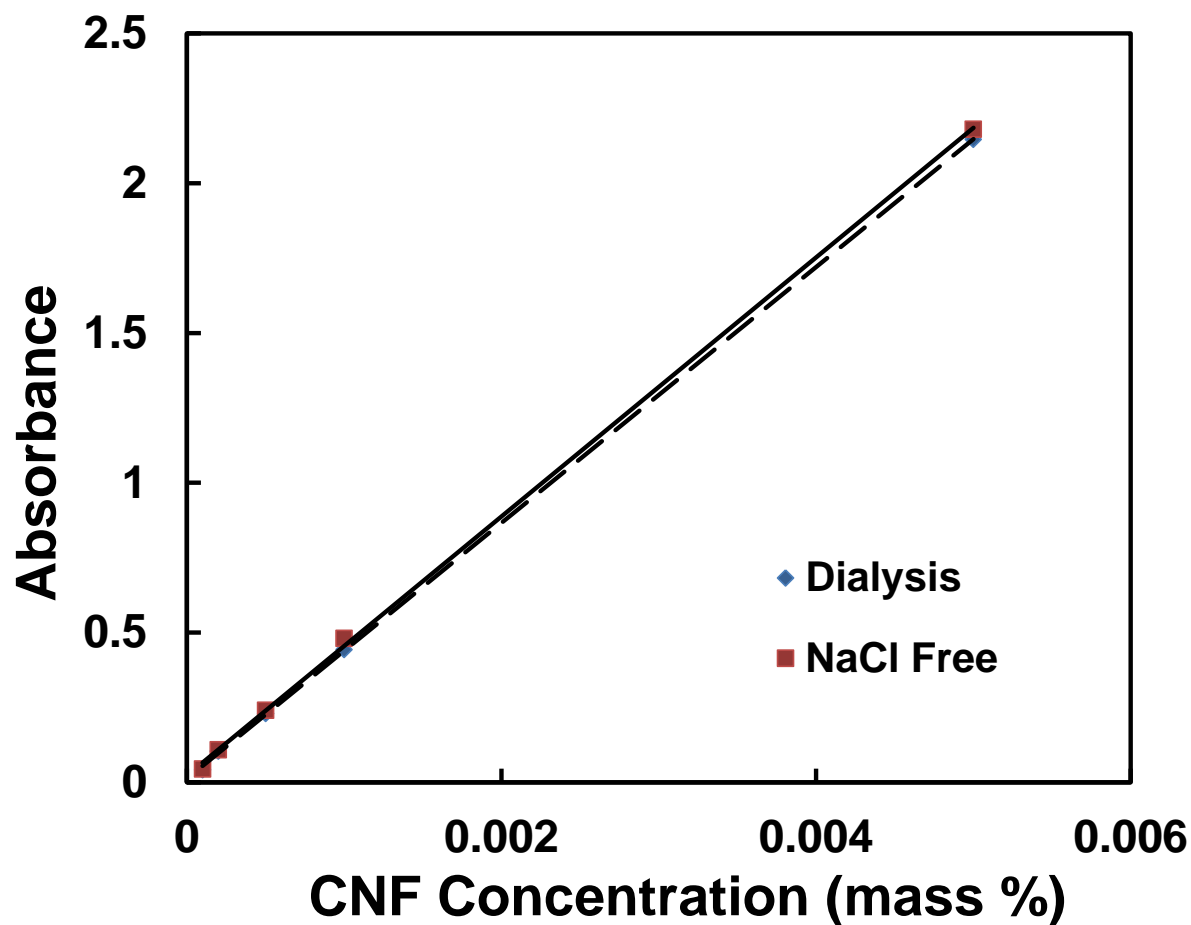


**FIGURE 2.** Beer's Law curve constructed from the measured absorbance at 267 nm from 5 CNF calibration standards obtained by dilution of a master suspension having a concentration of  $0.005 \pm 0.0003$  mass %. The  $2\sigma$  standard uncertainty of the repeated measurements is smaller than the data markers.

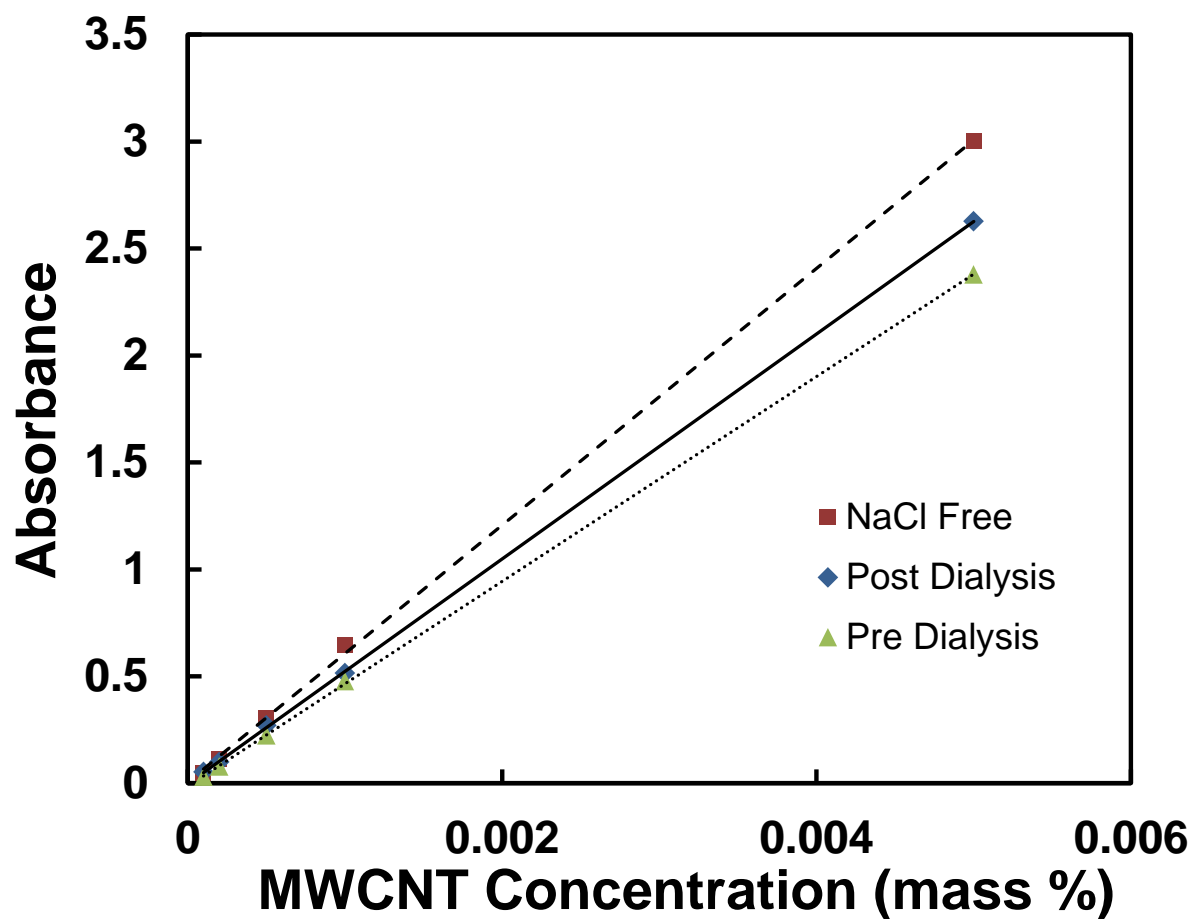


**FIGURE 3.** Beer's Law curve constructed from the measured absorbance at 267 nm from 5 MWCNT calibration standards obtained by dilution of a master suspension having a concentration of  $0.005 \pm 0.0003$  mass %. The  $2\sigma$  standard uncertainty of the repeated measurements is smaller than the data markers.

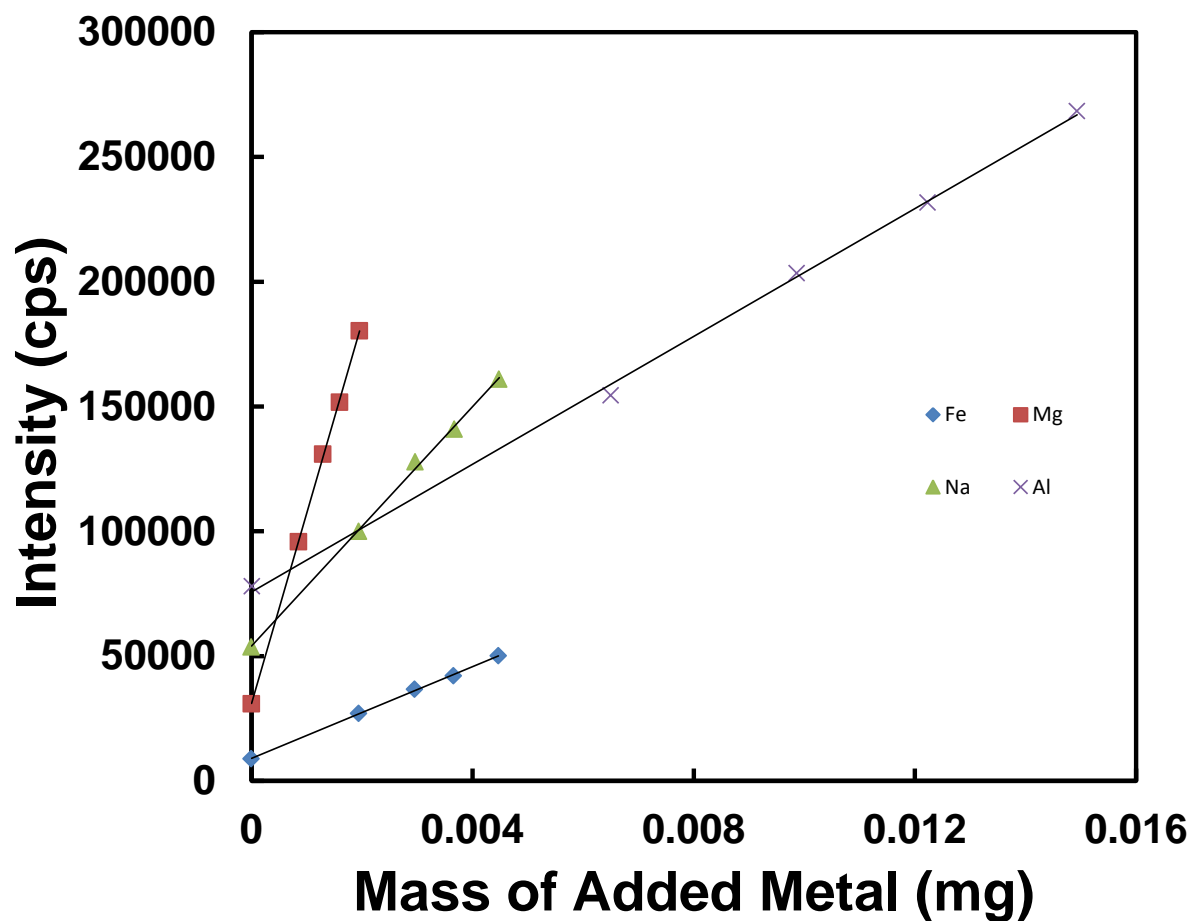


**FIGURE 4.** ICP-OES intensities as a function of the amounts of Al, Fe, Mg, and Na added to a dilute nitric acid/DI solution containing  $0.002 \pm 0.0001$  mass % MMT. The  $2\sigma$  standard uncertainty of the repeated measurements is smaller than the data markers.

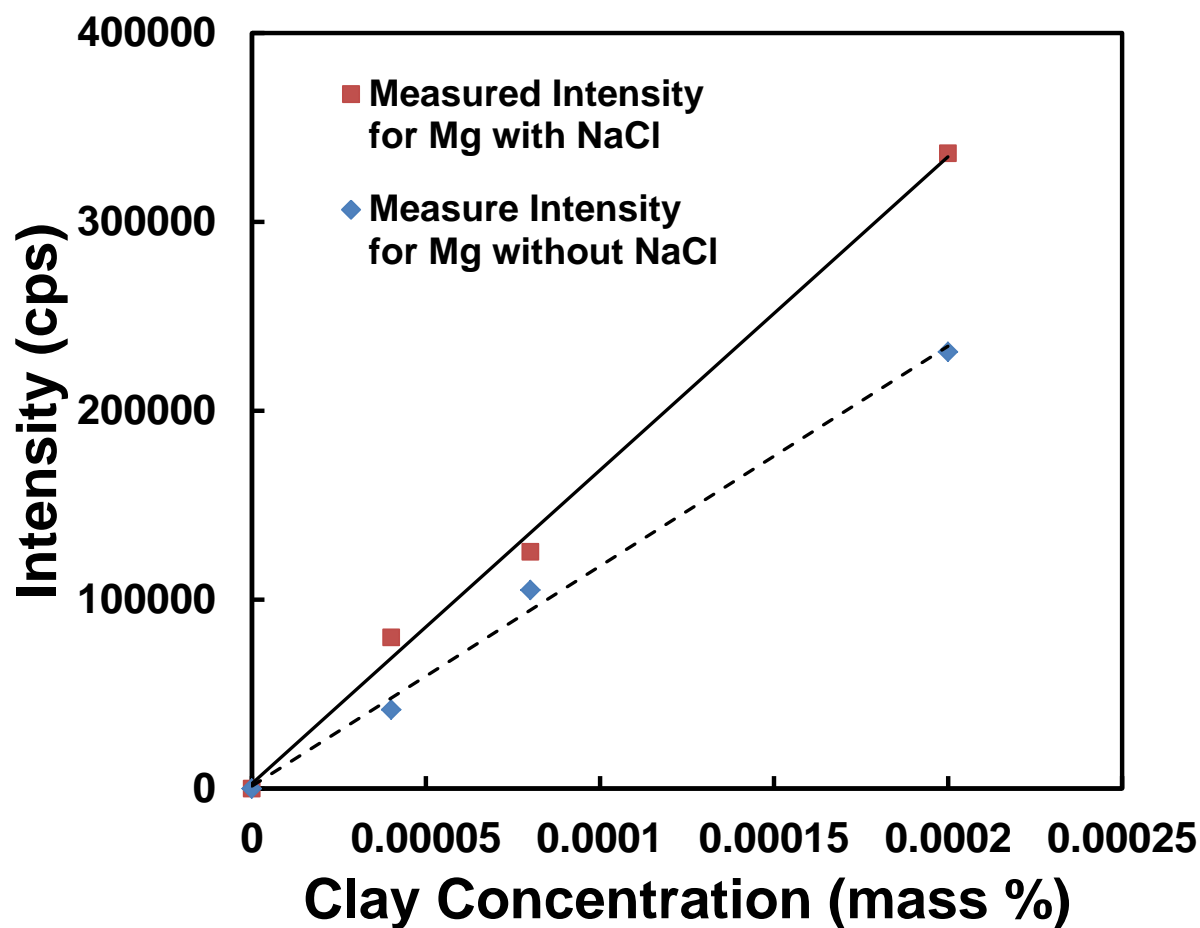


**FIGURE 5.** Calibration curves relating ICP-OES intensity to MMT concentration (for solutions with and without 0.2 % NaCl). The  $2\sigma$  standard uncertainty of the repeated measurements is smaller than the data markers.

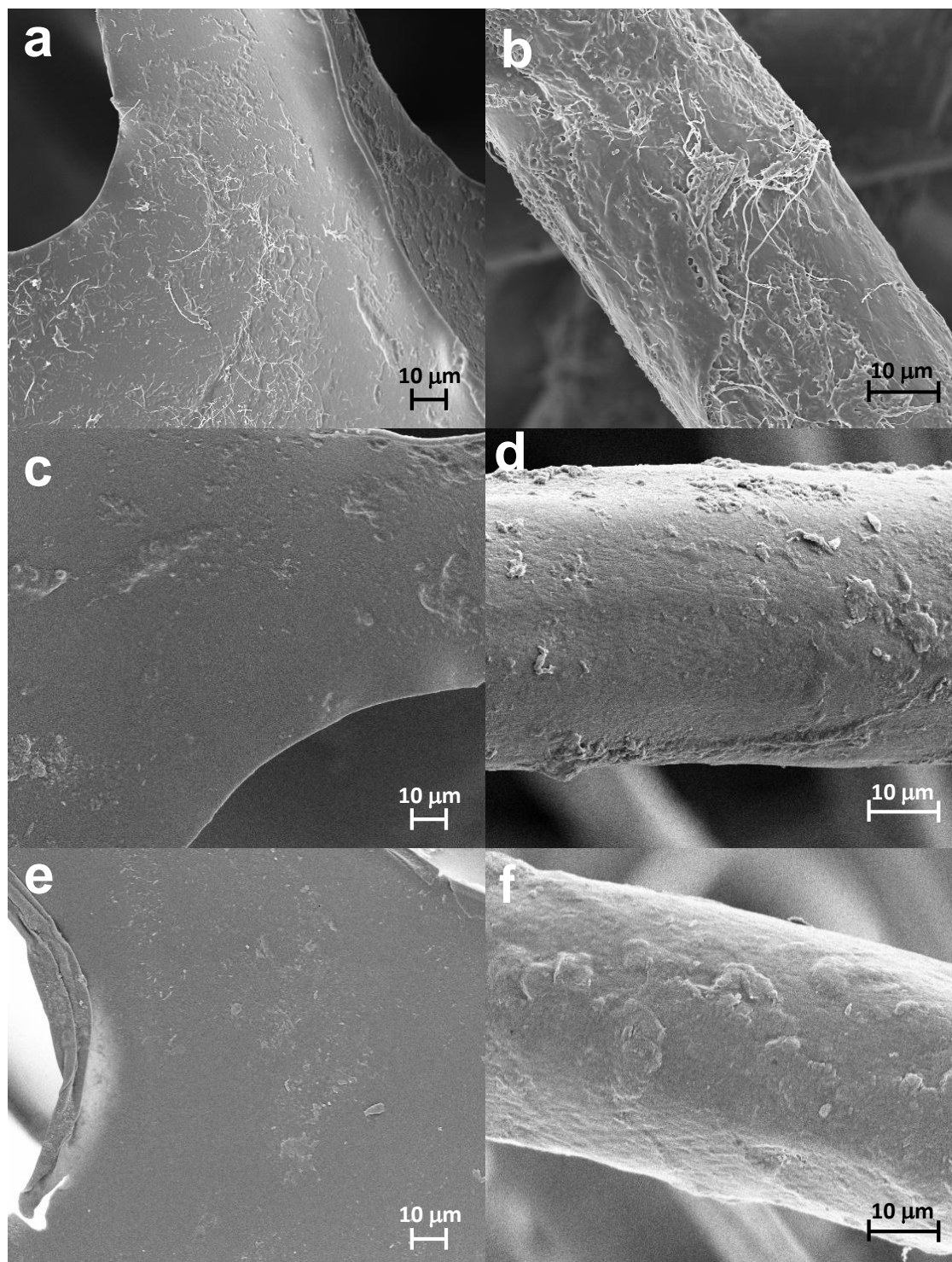


**FIGURE 6.** SEM images of CNFs on polyurethane foam (a) and barrier fabric (b), MWCNTs on polyurethane on foam (c) and barrier fabric (d), and MMTs on polyurethane foam (e) and barrier fabric (f). All images were capture before stressing.

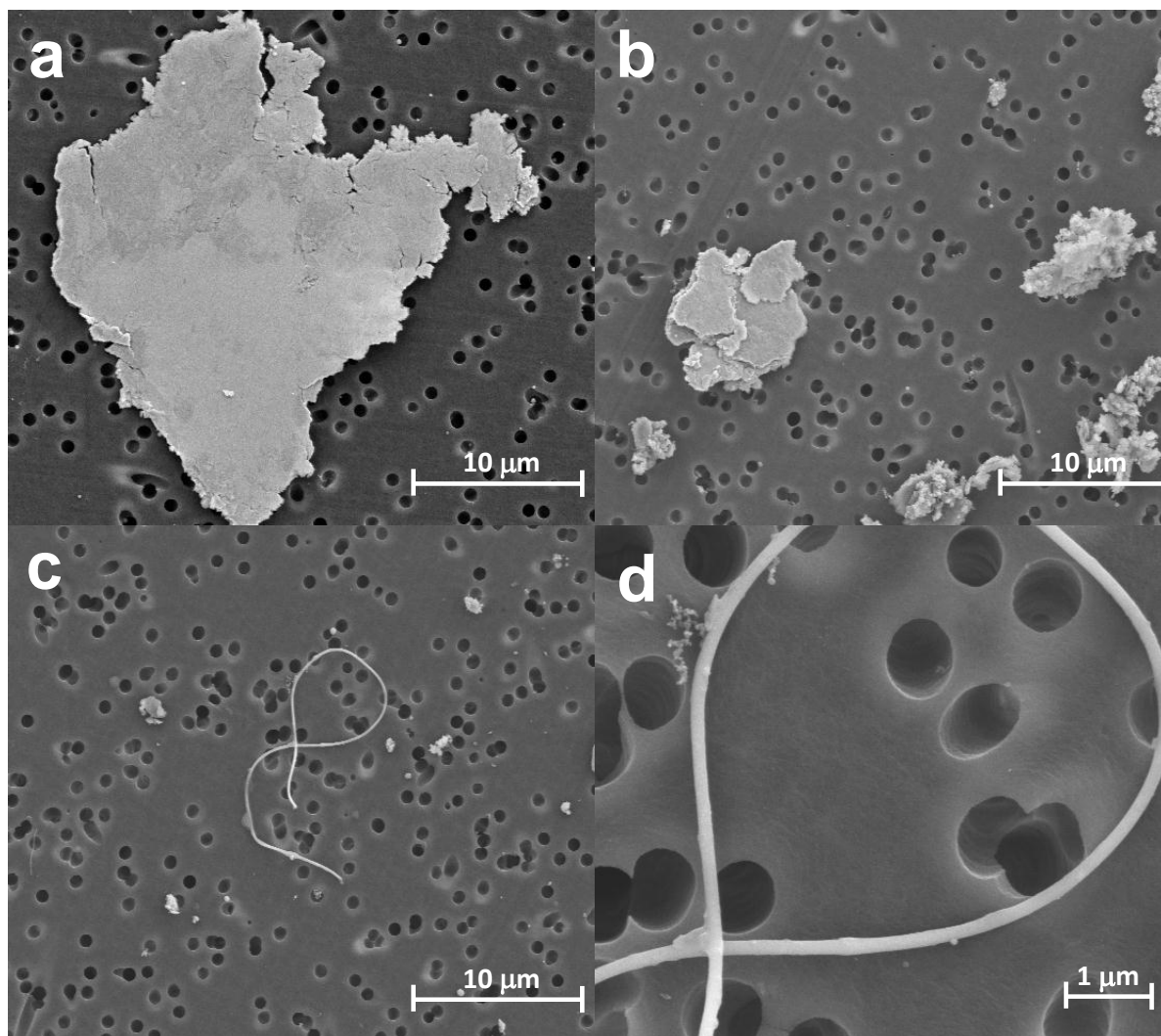


**FIGURE 7.** Released particles due to the mechanical pounding from MMT coating (a), MWCNT coating (b), and CNF coating (c) and (d). All samples were collected from the coatings applied on the polyurethane foam.

TABLE I. Nanoparticles released in the wear and tear experiments

<b>Substrate</b>	<b>Absorbance/Emission Intensity</b>	<b>Mass fraction % of total nanoparticle content</b>	<b>Mass per specimen (mg)</b>
CNF/BF	0.187	$0.0400 \pm 0.00020$	$0.0370 \pm 0.00185$
MWCNT/BF	0.157	$0.0270 \pm 0.00135$	$0.0250 \pm 0.00125$
MMT/BF	30583	$0.0009 \pm 0.000045$	$0.0024 \pm 0.00012$
CNF/PUF	0.116	$0.0100 \pm 0.00050$	$0.0210 \pm 0.00105$
MWCNT/PUF	0.120	$0.0085 \pm 0.000425$	$0.0190 \pm 0.00095$
MMT/PUF	18577	$0.00028 \pm 0.000014$	$0.00095 \pm 0.00004$

*Note:* values are reported with  $2\sigma$  standard uncertainty

TABLE II. Nanoparticles released in the simulated chewing experiments

<b>Substrate</b>	<b>Absorbance/Emission Intensity</b>	<b>Mass fraction % of total nanoparticle</b>	<b>Mass per specimen (mg)</b>
CNF/BF	0.239	$0.140 \pm 0.007$	$0.0140 \pm 0.0007$
MWCNT/BF	0.879	$0.420 \pm 0.021$	$0.0460 \pm 0.0023$
MMT/BF	546132	$0.130 \pm 0.0065$	$0.0370 \pm 0.0018$
CNF/PUF	0.0780	$0.053 \pm 0.0027$	$0.0052 \pm 0.00026$
MWCNT/PUF	0.723	$0.460 \pm 0.023$	$0.0470 \pm 0.0023$
MMT/PUF	62680	$0.043 \pm 0.0026$	$0.0054 \pm 0.00027$

*Note:* values are reported with  $2\sigma$  standard uncertainty